

Assessment of Spatial Resolution on SPECT using Image Processing

Einas M. Ahmed, Suhaib Alameen, YousraKhairi, Mohamed E. M. Gar-Elnabi

¹*Sudan University of Science and Technology. College of Medical Radiological Sciences P.O.Box 1908, Khartoum, Sudan*

Abstract: *The main objective of this study to assess the spatial resolution of SPECT gamma camera using developed Algorithm via image processing procedure. Usually assessment done through visual inspection of phantom images i.e. visual perception trend; in this study, separate algorithm was developed using Interactive Data Language IDL software to quantify the resolution with Modulation Transfer Function (MTF). The data were collected from Departments of nuclear medicine in main hospitals in Khartoum – Sudan (RCIH & RICK) in period from 2015 to 2017; images of QC test were taken from SPECT gamma camera as DICOM format. The result showed that the resolution for minimum object used 4mm was 70% and increased with object size increased to reach 100% resolution for an object size of 10 mm i.e. 100% resolution corresponds to the coordinate of the MTF at 10% and frequency of 0.05cycle /mm. Inconclusion the developed algorithm can be used objectively and improved as required without looking for expertise from other country, as well it can be made to check the acceptance of the device performance regardless the built-in programs.*

Keywords: *Resolution, SPECT, MTF, Image Processing*

I. Introduction

Single photon emission computed tomography (SPECT) has been used for three-dimensional displays of radioactive distributions and for estimating volumes within the body [1,2]. However, SPECT values do not always represent true radioactive concentrations, thus quantitative analyses are rendered unreliable. These facts can be explained by several factors, such as projection data acquisition, reconstruction of transverse images, absorption correction, Compton scattering, energy resolution, and image noise [3-5]. Limited spatial resolution, which is dependent on source-detector distance, may also play a role. The effect of spatial resolution was studied for positron emission tomography (PET) [6-8]. It has been shown that object sizes obtained with true radioactive concentrations were 2 x full width at half maximum (FWHM), 2.4 x FWHM, and 2.7 x FWHM for one-, two-, and three-dimensional objects for hot regions [8]. For SPECT, the relationship soft he recovery coefficient (RC) to the hot source area were studied for various collimators and image reconstruction filters, using technetium-99m (^{99m}Tc) and indium-131 (¹³¹In) [9].

Intrinsic spatial resolution

This is defined as the full-width at half-maximum (FWHM) of a line spread function (LSF) or of a point spread function (PSF) without an imaging collimator installed. This measurement should be supplemented by the full-width at tenth-maximum (FWTM) as the PSF or LSF may deviate from a Gaussian profile. Standard methodologies for LFOV gamma cameras [10,11,12,13] use a capillary line source of approximately 40MBq activity, of internal diameter of 0.5 mm. This is positioned parallel to the principal orthogonal axes of the camera to avoid broadening of the LSF. the source is placed directly on top of the uncollimated scintillator crystal. The intrinsic resolution of a LFOV gamma camera is typically in the region of 3 mm [14]. If an imaging matrix of 256_256 pixels is used, the pixel dimension of a 540 mm diameter gamma camera (to choose a single example) will be around 2.1 mm. NEMA NU1-2007 [10] states the “pixel size should be less than or equal to 0.1 FWHM”, that is 0.3 mm for a 540 mm diameter gamma camera. To achieve the specified “pixel size” the analogue to digital conversion gain is increased perpendicular to the line source for each orthogonal axis simultaneously, and the “zoomed” portion of the field of view is imaged. SFOV cameras have reported values of spatial resolution of less than 1.0 mm [15,16,17,18], suggesting that the NEMA “pixel size” should be at most 0.1 mm (equal to 0.1 FWHM). For a typical LFOV resolution of 3 mm, the use of a 0.5 mm line source will not have a large effect on measured resolution; at submillimeter resolution, however, the width of the same source becomes significant. Following the standards for LFOV systems, line source width (or the diameter of the point source) would need to have dimensions less than 0.1 mm. the uniform filling of capillary tubes with diameters of the order 100 mm is difficult to achieve. On this scale, even the manufacture of a slit transmission phantom becomes challenging. This method of intrinsic spatial resolution measurement is therefore not suitable for high-resolution SFOV systems. An alternative derivation of the FWHM can be obtained using the edge response function (ERF) method [10,19]. This can be obtained using a mask with a machined edge. When irradiated with a uniform radioactive source such that incident gamma photons can be assumed to be perpendicular to the mask

plane, the detected counts across the edge of the mask ideally correspond to a stepfunction, the derivative of which gives a LSF [19] which may then be analyzed as in LFOV protocols.

System spatial resolution

This is defined as the FWHM of a LSF or of a PSF with the imaging collimator in place. the protocol for LFOV gamma cameras uses a capillary line source (internal diameter less than 0.5 mm) with FWHM response measured in air and with scattering media (such as Perspex) positioned between the line source and the collimator surface [10].The Perspex acts to scatter photons as would be expected from a source inside a patient. Typically, LFOV system resolution measurements are stated in the context of the collimator used either at the collimator face or at a known distance (usually 100 mm) away from the collimator. System resolution is typically limited by the type of collimator used rather than the intrinsic resolution of the detector.

Similar to intrinsic resolution measurements, for SFOV cameras the line source width or point source diameter would ideally be smaller than that used for LFOV measurements, again proving difficult to manufacture and fill [20]. The benefit of a consistent approach across all gamma cameras outweighs the effects of a finite source and the standard LFOV method, with a 0.5 mm diameter line source, may be used. It may be possible to use a point or line source of a known diameter and then deconvolve the expected profile from the resultant image to determine the resolution; this is not ideal and requires specific knowledge of the expected profile of the source [21] and so may produce inconsistent results for different systems. Many SFOV cameras use pinhole collimators rather than the more widely used parallel-hole collimator. This means that a line source imaged at the collimator face would appear to be a flood source in the resultant image. Instead of reporting resolution at the collimator face, measurements for pinhole systems should be stated at the non-magnifying point. As resolution varies significantly with aperture to source distance (through scattering material), the relationship between these two factors should also be reported so that resolution may be calculated by the end user for any source distance. The measurement of camera intrinsic resolution and linearity are performed simultaneously using a dedicated lead mask with 1-mm slits spaced every 30 mm in the X or Y direction. The analysis of intrinsic resolution involves calculation of the full width at half maximum (FWHM) and the full width at tenth maximum (FWTM) for each of a series of profiles drawn across the slit lines. The mean, maximum, and minimum values for the set of profiles are then determined. Linearity assessment requires calculation of the deviation of the maximum value of the profile across each line and over the whole surface of the camera.

II. Material and Methods

Nucline Spirit DH-V machine used in this study. The average energy of Nucline Spirit 230V/50HZ and weight 2,100 (4,620) kg Thickness, 9.5 (3/8) mm (in) (detector characteristics) with power needed 230 VAC, 15 A; 110 VAC, 30 A. The machine is hole body scan, DIMENSIONS (HXWXD), CM (IN) (detection process, HR) 165 x 145 x 120 (65 x 57 x 47), The Collimators is LEGP, LEHR, LEUHR, MEGP, HEGP data input at camera station Intel Pentium 4, 3.06 GHz.

Resolution Assessment:

The performance of a scintillation camera system must be assessed each day of use to assure the acquisition of diagnostically reliable images. Performance can be affected by changes or failure of individual system components or subsystems and environmental conditions such as electrical power supply fluctuations, physical shock, temperature changes, humidity, dirt, and background radiation.



Fig 1. gamma camera with a quadratic bar phantom placed on top of the gamma camera detector



Fig2. gamma camera with a quadratic bar phantom placed on top of the gamma camera detector and radioactive source on top of the quadratic phantom for transmission images

Resolution recently defined as the degree of smearing of an object image and traditionally it measured as the size of the FWHM of the image for line transfer function (LTF) in pixel then this pixel converted to mm by multiplying the number of pixel by the size of one pixel in mm, then divide the original by the measured value and multiply by 100. This method introduces some errors due to Dot Per Inch (DPI) approximation which depend on the image mapping process. Application of Modulation Transfer Function (MTF) will solve this problem, where the LTFs were transformed into frequency domain, then absolute value were taken to remove the negative frequencies (mirror) and then divide the frequency domain values by the maximum value and multiply by 100 to get MTF in percentage were depicted in the y-axis then in the x-axis the values of the real image bars values converted into frequency using the following equation $f = 1/2\Delta$ where Δ is the size of the object in mm. Resolution frequency in cycle/mm will in nuclear medicine (gamma camera) will correspond to 10% MTF, then the cycle can be converted to mm to find the resolution as in the method of FWHM as shown in the algorithm below.

III. Results

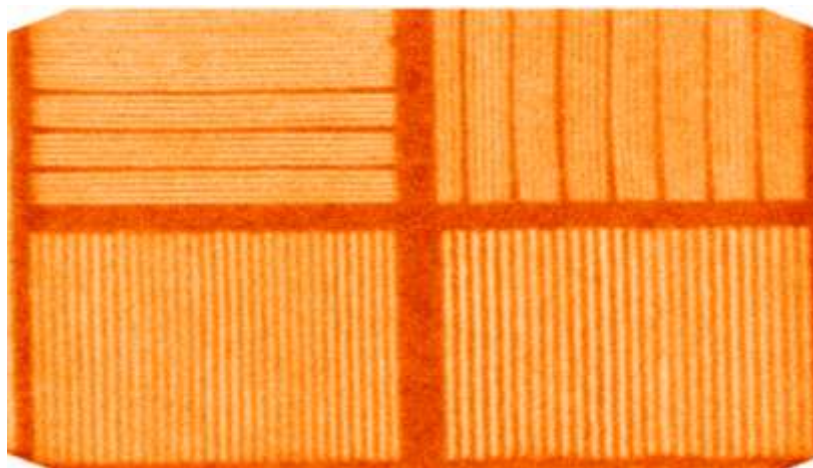


Fig 3.Gamma camera image for a quadratic bar phantom with different slits size to measure the resolution

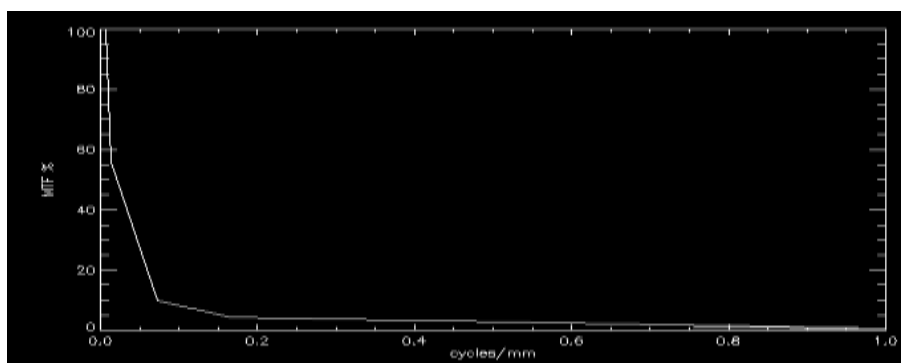


Fig4. a line graph show modulation transfer function of the different thickness of the quadratic phantom versus frequencies of the slits size to find the resolution frequency of gamma camera at 10% MTF.

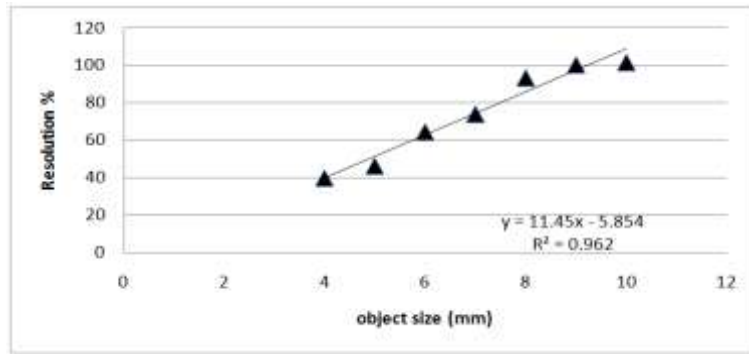


Fig 5. Scatter plot of the object size (size of the slit) versus resolution, it shows a direct linear relationship.

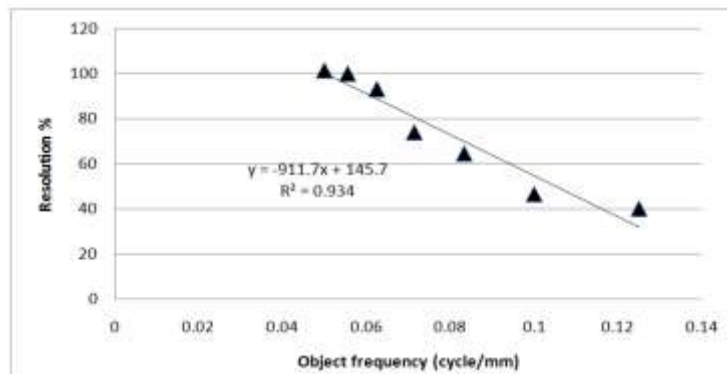


Fig 6. scatter plot of the object frequency (frequency of the slit size) versus resolution, it shows an indirect linear relationship.

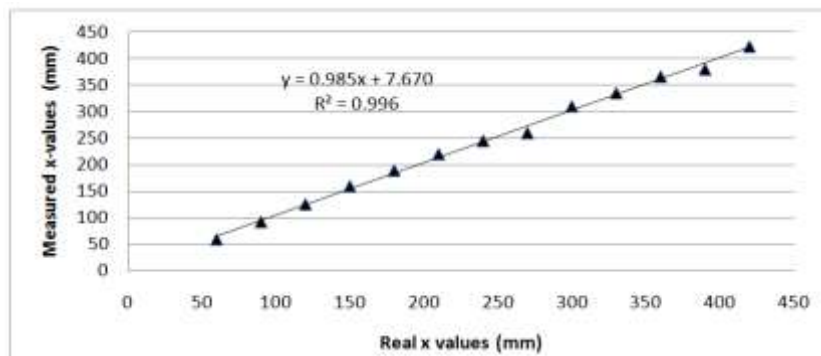


Fig 7. scatter plot shows a direct linear relationship between the real locations of the slits in the phantom and the central peaks of the counts in the vertical image that corresponds to the real location by fitting a curve on the line spread function graph

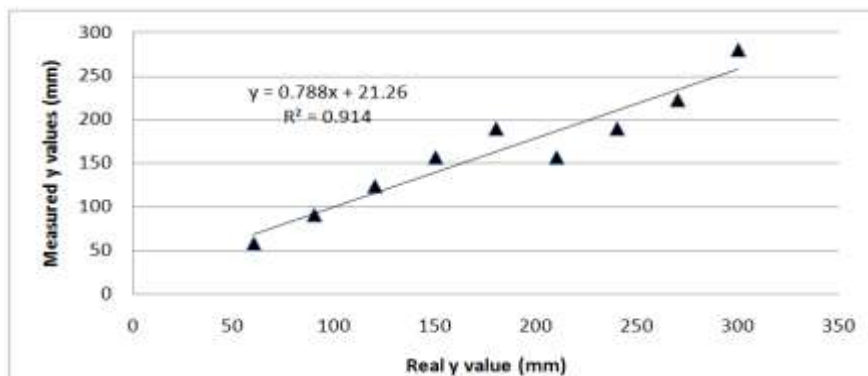


Fig 8. scatter plot shows a direct linear relationship between the real locations of the slits in the phantom and the central peaks of the counts in the horizontal image that corresponds to the real location by fitting a curve on the line spread function graph

IV. Discussion

The spatial resolution of the Gamma camera increases with an object size (mm) increases (Fig 5.) The resolution for minimum object used 4mm was 70% and increased with object size increased to reach 100% resolution for an object size of 10 mm i.e. Resolution = 11.45%/mm of object size. Resolution also could be measured using MTF making benefit of frequency domain properties; where the resolution of gamma camera usually corresponds to frequency that match 10% of MTF value in gamma camera images. In this study as shown in graph 6. there is indirect linear relationship between the frequency of the object and resolution; which means the resolution decreases as the object frequency increases because the increases of frequency means decrease of object size and vice versa, the linear scatter plot reveals that the resolution % decrease by 911.7%/cycle /mm; also, the graphs showed that the resolution which correspond to the coordinate of the MTF at 10% and frequency of 0.05cycle /mm.

V. Conclusion

The result of RICK camera represents 10% resolution at object frequency 0.05 and 0.06 while the result of RICH camera showed 10% resolution at object size of 0.05 gives 100%

Reference

- [1] Budinger TF, Guilberg GT. Three dimensional reconstruction in nuclear medicine emission imaging. *IEEETransNucl Sci* 1974; NS-2 1:2-20.
- [2] StraussLG, Clorius JH, Frank T, Kaick GV. Single photon emission computerizedtomography(SPECT) for estimatesof liver and spleen volume. *J Nucl Med* 1984;25:81-85.
- [3] Budinger TF. Physical attributes of single-photon tomography.*JNuclMed* 1980;21:579-592.
- [4] Moore SC. Quantitative capabilities of single-photon emission computerized tomography. In: MagiStretti FL, ed. *Functionalradionuclideimagingofthe brain*. New York:Raven Press,1983:177-192.
- [5] Soussaline FP, Todd-Pokropek AE, Zurowski 5, Huffer E, RaynaudCE, KellershojnCL. A rotatingconventional gamma camera single-photon tomographic system: physical characterization. *J Comp Assist Tomogr*1981;5:551-556.
- [6] HoffmanEJ, HaungSC, PhelpsME. Quantitationin positron emission computed tomography: 1. effect of object size. *J Comp Assist Tomogr* 1979; 3:299-308.
- [7] Mazziotta JC, Phelps ME, Plummer D, KuhlDE.Quantitation in positron emission computed tomography: . physical-anatomical effects. *J Comp Assist Tomogr*1981;5:734-743.
- [8] KesslerRM, EllisJR. Jr.,EdenM. Analysisofemissionsiontomographicscan data: limitations imposed by resolution and background. *J Comp Assist Tomogr*1984;8:514-522.
- [9] ClarkeLP, LeongLL,SerafiniAN, Tyson IB.SilbigerML.QuantitativeSPECTimaginginfluenceof object size. *Nuci Med Commun* 1986; 7:363-3
- [10] Chapman J, Hugg J, Vesel J, Bai C, Bleviss I, Barrett H, et al. Performance measurement of scintillation cameras. Rosslyn, VA: National Electrical Manufac- turers Association; 2007. NEMA NU 1.
- [11] Bolster A, Hannan J, Cosgriff PS, Mostaffa AB, Parkin A, Sharp PF, et al. In: Bolster A, editor. Report 86 Quality assurance in gamma camera systems. York: Institute of Physics and Engineering in Medicine; 2003, ISBN 1 903613,13 2, p. 1e130.
- [12] BusemannSokole E, Plachćinska A, Britten A, Lyra Georgosopoulou M, Tindale W, Klett R. Routine quality control recommendations for nuclear medicine instrumentation. *Eur J Nucl Med Mol Imaging* 2010;37:662e71.
- [13] BusemannSokole E, Plachćinska A, Britten A. Acceptance testing for nuclear medicine instrumentation. *Eur J Nucl Med Mol Imaging* 2010;37:672e81.
- [14] Vesel J, Petrillo M. Improved gamma camera performance using event positioning method based on distance dependent weighting. *IEEE Nucl Sci Conf R* 2005;5:2445e8.
- [15] Porras E, Escat B, Benlloch JM, Kadi-Hanifi D, Lopez S, Pav_on N, et al. Portable mini gamma camera for medical applications. *NuclInstrum Meth A* 2002;486: 186e90.
- [16] De Vree GA, Westra AH, Moody I, van der Have F, Ligtoet KM, Beekman FJ. Photon-counting gamma camera based on an electron-multiplying CCD. *IEEE Trans Nucl Sci* 2005;52:580e8.
- [17] Fiorini C, Longoni A. Gamma-ray imaging detectors based on silicon drift detectors arrays coupled to a single scintillator. *NuclInstrum Meth A* 2003;497:221e5.
- [18] Tsuchimochi M, Sakahara H, Hayama K, Funaki M, Ohno R, Shirahata T, et al. A prototype small CdTe gamma camera for radioguided surgery and other imaging applications. *Eur J Nucl Med Mol Imaging* 2003;30:1605e14.
- [19] V-ayrynen T, Pitk € anen U, Kiviniitty K. Methods for measuring the modulation transfer function. *Eur J Nucl Med* 1980;5:19e22.
- [20] Lees JE, Bassford DJ, Blackshaw PE, Perkins AC. Design and use of mini-phantoms for high resolution planar gamma cameras. *ApplRadiatIsot*2010;68:2448e51.
- [21] Lees JE, Bassford DJ, Blake OE, Blackshaw PE, Perkins AC. A high resolution small field of view (SFOV) gamma camera: a columnar scintillator coated CCD imager for medical applications. *J Instrum*2011;6:1e12.